ELSEVIER

Journal of Power Sources 81–82 (1999) 589–593

JOURNAL OF POWER SOURCES

www.elsevier.com/locate/jpowsour

Synthesis and characterization of $LiAl_yCo_{1-y}O_2$ and $LiAl_yNi_{1-y}O_2$

Young-Il Jang [a], Biying Huang [a], Haifeng Wang [a], Garry R. Maskaly [a], Gerbrand Ceder [a], Donald R. Sadoway [a], Yet-Ming Chiang [a,*], Hui Liu [b], Hirokazu Tamura [b]

[a] *Department of Materials Science and Engineering, Massachusetts Institute of Technology, Cambridge, MA 02139, USA*
[b] *Furukawa Electric, Yokohama Research Center, Yokohama 220, Japan*

Abstract

Aluminum is of interest as a constituent in Li secondary battery cathodes due to its low cost and low mass. Increased intercalation potential for certain Al-doped intercalation oxides has also been predicted by ab initio calculations. We have synthesized single phase $LiAl_yCo_{1-y}O_2$ and $LiAl_yNi_{1-y}O_2$ solid solutions from homogeneous hydroxide precursors. In $LiAl_yNi_{1-y}O_2$, it was found that the addition of $LiAlO_2$ helps to stabilize $LiNiO_2$ in the α-$NaFeO_2$ structure during air firing, facilitating preparation of the ordered phase. A systematic increase in the open circuit voltage is observed with Al content in both $LiAl_yCo_{1-y}O_2$ and $LiAl_yNi_{1-y}O_2$ solid solution, providing additional support for the ab initio calculations.

Keywords: Lithium batteries; Cathodes; Lithium cobalt oxide; Lithium nickel oxide

1. Introduction

Compounds $LiMO_2$ (M = Co [1], Ni [2]), having the α-$NaFeO_2$ structure (space group $R\bar{3}m$), have been extensively studied as cathodes for Li-ion batteries. The effect of doping with other transition metal elements have also been studied [3–5]. Compared with the transition metals, Al has not received wide attention as a dopant, with only a few reports on $LiAl_yM_{1-y}O_2$ (M = Co, Ni) systems to date [6–8]. However, doping with Al has gained in interest for several reasons. Ab initio calculations by Aydinol et al. [9] have shown that $LiAlO_2$ has a theoretical intercalation voltage of $\sim$5 V vs. Li/Li^+, which is higher than that of any lithium transition-metal oxide. While pure $LiAlO_2$ is electrochemically inactive, the solid solution of $LiAlO_2$ with lithiated transition-metal oxides can potentially increase the intercalation voltage. This effect has recently been verified for $LiAl_yCo_{1-y}O_2$ solid solutions [10]. Secondly, the fact that $LiAlO_2$ is stable in the α-$NaFeO_2$ structure at temperature below $\sim$600°C [11] suggests that it could have a stabilizing effect of the structure when doped into other compounds. This effect has recently been demonstrated for monoclinic $LiAl_yMn_{1-y}O_2$ [12]. Finally, its low cost and low density makes $LiAlO_2$ attractive as an intercalation compound constituent. In this paper, we report on the experimental investigation on the effect of Al on the structure and electrochemical properties of $LiCoO_2$ and $LiNiO_2$.

2. Experimental

$LiAl_yCo_{1-y}O_2$ and $LiAl_yNi_{1-y}O_2$ samples were synthesized by firing homogenous precursor powders obtained by a co-precipitation and freeze-drying technique [13]. Mixed aluminum–cobalt or aluminum–nickel hydroxides were co-precipitated from mixed aqueous solutions of $Al(NO_3)_3 \cdot 9H_2O$ and $Co(NO_3)_2 \cdot 6H_2O$ or $Ni(NO_3)_2 \cdot 6H_2O$, respectively. A more detailed description of precursor preparation can be found elsewhere [13]. Precursors thus obtained for $LiAl_yCo_{1-y}O_2$ and $LiAl_yNi_{1-y}O_2$ were fired for 2 h at 700–800°C in air or oxygen, respectively. To compare the characteristics of this chemically prepared, highly homogeneous precursor with a simpler preparation of the same components, limited experiments were also conducted to synthesize $LiAl_yNi_{1-y}O_2$ using commer-

* Corresponding author

0378-7753/99/$ - see front matter
PII: S0378-7753(99)00104-4

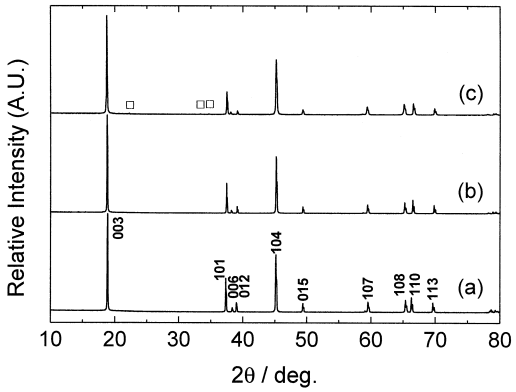

Fig. 1. XRD patterns for $LiAl_yCo_{1-y}O_2$ obtained after firing for 2 h at 800°C in air for (a) $y = 0$, (b) $y = 0.25$ and (c) $y = 0.5$, with *hkl* indicated for $LiCoO_2$ (□ γ-$LiAlO_2$).

cially available $Al(OH)_3$, $Ni(OH)_2$ and Li_2CO_3, which were mixed by ball-milling in a polypropylene container using alumina milling media and then calcined at 800°C for 24 h in air. All samples were furnace-cooled to room temperature after firing. Calcined powders were characterized by TEM, STEM/EDX and X-ray diffraction (XRD) using Cu-K_α radiation. In this paper, electrochemical test results are for chemically synthesized materials unless otherwise noted.

For electrochemical evaluation, oxide powders were mixed with carbon black, graphite and poly(vinylidene fluoride) (PVDF) in the weight ratio of 78:6:6:10. The electrochemical test cell consisted of two stainless steel electrodes with a Teflon holder. Lithium ribbon of 0.75 mm in thickness was used as the anode. The separator was a film of Celgard 2400™, and the electrolyte consisted of a 1 M solution of $LiPF_6$ in ethylene carbonate (EC) and diethyl carbonate (DEC). The ratio of EC to DEC was 1:1 by volume. Additional details of electrochemical testing are discussed elsewhere [14]. Three-electrode electrochemical cells were also used to measure open circuit voltage (OCV). In these cells, the working electrode was the $LiAl_yCo_{1-y}O_2$ composite electrode, and counter and reference electrodes were Li. The reference electrode and working electrode were separated from the counter electrode by a PVDF membrane. The electrolyte was 1 M $LiClO_4$ in EC and dimethyl carbonate (DMC). The ratio of EC to DMC was 1:1 by volume.

3. Results and discussion

3.1. $LiAl_yCo_{1-y}O_2$

XRD patterns of $LiAl_yCo_{1-y}O_2$ for $y = 0$, 0.25 and 0.5 are shown in Fig. 1a–c, respectively. All samples are single phase and have the α-$NaFeO_2$ structure, space group $R\bar{3}m$. Miller indices (*hkl*) are indexed for $y = 0$ in the hexagonal setting. Peaks for the γ-$LiAlO_2$ phase (tetragonal) are barely distinguishable at $y = 0.5$ (Fig. 1c), indicating that the solid solubility limit is exceeded at $y \cong 0.5$ at 800°C. The solid solubility limit in our samples is higher than that reported by Nazri et al. [8] (~25% at 750°C). Still higher solubility may be obtainable at higher firing temperature. Upon increasing Al content, the (006) and (108) peaks shift toward lower 2θ angles, resulting in a wider split of (006)/(012) and (108)/(110) peaks compared with $LiCoO_2$. The lattice parameters calculated by a least squares method from the XRD data are $a = 2.816$, 2.809, 2.806 Å and $c = 14.049$, 14.115, 14.150 Å for

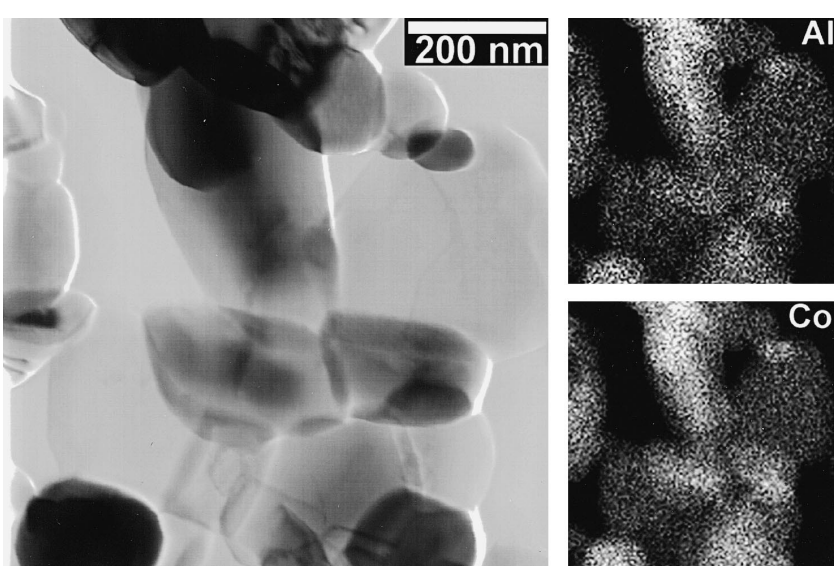

Fig. 2. STEM/EDX elemental maps for Al and Co in $LiAl_{0.5}Co_{0.5}O_2$ obtained after firing for 2 h at 800°C in air.

$y = 0$, 0.25, 0.5, respectively. Substitution of Al results in shorter a and larger c, increasing the c/a ratio from 4.99 for $y = 0$ to 5.04 for $y = 0.5$. Fig. 2 shows direct observation and energy-dispersive X-ray mapping of the oxide powder particles with scanning transmission electron microscopy, confirming that the Al and Co are uniformly distributed throughout the particles.

The ab initio calculations give the equilibrium potential of $LiAl_yCo_{1-y}O_2$ averaged over a certain Li concentration range [9,10]. Complete intercalation curves have also recently been computed [15]. However, exact measurement of the equilibrium potential is difficult. We used the observable OCV measured as a close approximation to the equilibrium potential. The OCV of $LiAl_yCo_{1-y}O_2$ was first measured by charging the two-electrode cells at 0.05 mA/cm^2 to the desired Li content, then equilibrating for 15 h so that the rate of OCV change was less than 1 mV/h. Fig. 3 shows the OCV thus measured, as function of composition for samples calcined for 2 h at 800°C in air. Note that the OCV increases systematically with the Al content in oxide, verifying the ab initio calculations as mentioned earlier [10]. The three-electrode cells were charged and discharged at 0.25 mA/cm^2 at every 12.4 mA h/g and allowed to equilibrate for 10 h. The OCV as a function of Li content measured in this manner is also plotted in Fig. 3, and clearly agrees well with the two-electrode results.

Charge/discharge performance of $LiAl_{0.25}Co_{0.75}O_2$ fired at 800°C for 2 h in air was tested between 2.0 and 4.5 V at 0.4 mA/cm^2. During the first charge, 182 mA h/g was extracted at room temperature, while the discharge capacity was 127 mA h/g (energy density 488 W h/kg). Compared to undoped $LiCoO_2$ prepared by the identical method [13], greater capacity fade was observed as shown in Fig. 4. After 9 cycles, the discharge capacity decreased to 51% of the initial value. The mechanism of this rapid capacity fade for $LiAl_yCo_{1-y}O_2$ is presently unknown. Increased capacity was obtained at 55°C with capacity retention of 72% after 9 cycles. A related paper discusses electrochemical cycling induced defects studied by electron microscopy [16].

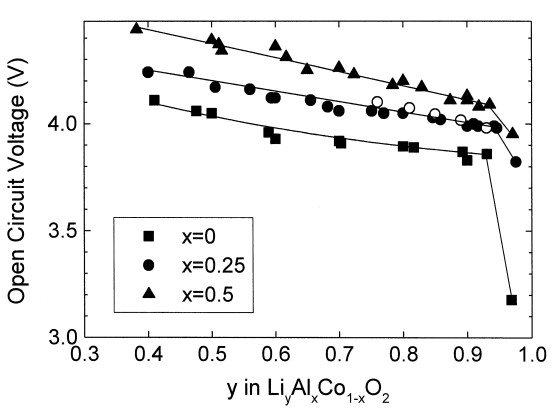

Fig. 3. OCV as a function of Li and Al content prepared by electrochemical oxidation of $LiAl_yCo_{1-y}O_2$. Symbol ○ represents data obtained using a three-electrode cell, as discussed in the text.

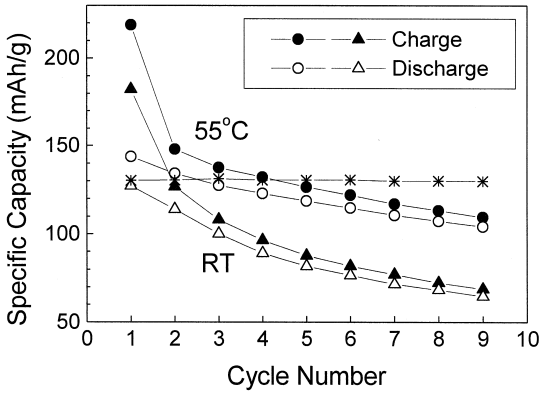

Fig. 4. Specific capacity vs. cycle number for $LiAl_{0.25}Co_{0.75}O_2$, tested against a Li metal anode at 0.4 mA/cm^2 between 2.0 and 4.5 V at room temperature and 55°C (* data obtained from undoped $LiCoO_2$).

3.2. $LiAl_yNi_{1-y}O_2$

XRD patterns of $LiAl_yNi_{1-y}O_2$ for $y = 0$ and 0.25 synthesized using simple physical mixtures of $Al(OH)_3$, $Ni(OH)_2$ and Li_2CO_3 are shown in Fig. 5a and b, respectively. Ball-milled precursor powders were fired for 24 h at 800°C in air. The sample corresponding to $y = 0$ exhibits a high (104)/(003) intensity ratio and no splitting of the (006)/(012) and (108)/(110) peaks, indicating that the obtained oxide has a highly disordered layered structure [17]. This result is consistent with the literature on undoped $LiNiO_2$ prepared under similar synthesis conditions

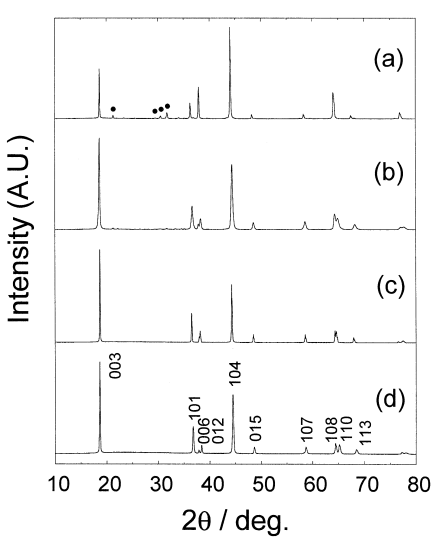

Fig. 5. XRD patterns for $LiAl_yCo_{1-y}O_2$. (a) and (b) correspond to oxide prepared by solid state reaction method (800°C, 24 h, air) for $y = 0$ and $y = 0.25$, respectively. (c) and (d) correspond to oxide prepared by co-precipitation method (700°C, 2 h, oxygen) for $y = 0$ and $y = 0.25$, respectively. *hkl* is indexed for a hexagonal setting in (d) (● Li_2CO_3).

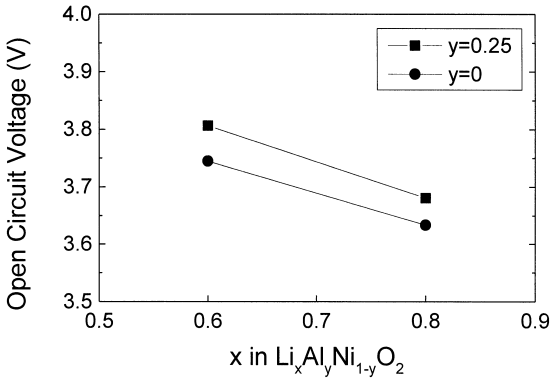

Fig. 6. OCV as a function of Li and Al content prepared by electrochemical oxidation of $LiAl_yNi_{1-y}O_2$.

[18,19]. Interestingly, the sample with $y = 0.25$ after firing under identical conditions shows a high $(003)/(104)$ intensity ratio and clear splitting of the $(006)/(012)$ and $(108)/(110)$ peaks, showing excellent layered cation ordering. Therefore, Al-doping is seen to stabilize α-$NaFeO_2$ cation ordering in $LiNiO_2$, allowing easier preparation of ordered material by firing in air. Interestingly, the amount of residual Li_2CO_3 also decreased for the Al-doped sample compared with the undoped one.

Fig. 5c–d show the XRD patterns of oxide powers obtained from co-precipitated precursor powders after firing for 2 h at 700°C in oxygen. Single phases of $LiNiO_2$ and $LiAl_{0.25}Ni_{0.75}O_2$ were obtained with well-ordered layered structure as indicated by high $(003)/(104)$ intensity ratios and clear splitting of the $(006)/(012)$ and $(108)/(110)$ peaks. As in $LiAl_yCo_{1-y}O_2$, upon adding Al, the (006) and (108) peaks shift toward lower 2θ angles, resulting in a wider split of $(006)/(012)$ and $(108)/(110)$ peaks compared with $LiNiO_2$. Comparing XRD patterns in Fig. 5a–b, it is noticeable that by using the homogeneous precursors obtained by co-precipitation, both the firing time and temperature necessary to obtain a highly ordered oxide are reduced. Note, however, that oxygen atmosphere was used for co-precipitated powders, whereas air was used for the ball-milled powders. Previous studies [20] have shown that firing in oxygen promotes synthesis of $LiNiO_2$ with α-$NaFeO_2$ cation ordering. Further experiments are underway in order to compare the processibility under identical firing atmosphere.

Preliminary electrochemical tests were conducted on the well-ordered $LiAl_yNi_{1-y}O_2$ prepared by the co-precipitation route. The OCV was measured by charging the cells at 0.1 mA/cm^2 to the desired Li content, then equilibrating for 15 h. Fig. 6 shows the OCV thus measured, for Al-doped and undoped $LiNiO_2$. Clearly, $LiAl_yNi_{1-y}O_2$ exhibits a higher OCV than undoped $LiNiO_2$. These results provide an additional confirmation, at least qualitatively, of the ab initio calculations [9,10]. Further investigation of the electrochemical properties of $LiAl_yNi_{1-y}O_2$ solid solutions and a more detailed comparison with theory is in progress.

4. Conclusions

$LiAl_yCo_{1-y}O_2$ and $LiAl_yNi_{1-y}O_2$ solid solutions that are well-ordered in the α-$NaFeO_2$ structure type have been synthesized. The open-circuit voltage increases with Al content in both systems, as was predicted by ab initio calculations [9,10]. Compared with $LiCoO_2$, a greater capacity fade rate was observed in $LiAl_yCo_{1-y}O_2$. Higher capacity and less capacity fade were observed at 55°C than at room temperature. In $LiAl_yNi_{1-y}O_2$, Al-doping has an additional effect of promoting the α-$NaFeO_2$ structure during firing in air, allowing the easier preparation of highly ordered materials.

Acknowledgements

This work was funded by Furukawa Electric and by the INEEL University Research Consortium. The INEEL is managed by Lockheed Martin Idaho Technology for the US Department of Energy, Idaho Operations Offices, under contract no. DE-AC07-94ID13223. We used instrumentation in the Shared Experimental Facilities at MIT, supported by NSF Grant no. 9400334-DMR.

References

[1] J.N. Reimers, J.R. Dahn, J. Electrochem. Soc. 139 (1992) 2091.
[2] J.R. Dahn, U. von Sacken, M.W. Jukow, H. Al-Janaby, J. Electrochem. Soc. 138 (1991) 2207.
[3] E. Rossen, C.D.W. Jones, J.R. Dahn, Solid State Ionics 57 (1992) 311.
[4] J.N. Reimers, E. Rossen, C.D. Jones, J.R. Dahn, Solid State Ionics 61 (1993) 335.
[5] R. Stoyanova, E. Zhecheva, L. Zarkova, Solid State Ionics 73 (1994) 233.
[6] T. Ohzuku, A. Ueda, M. Kouguchi, J. Electrochem. Soc. 142 (1995) 4033.
[7] Q. Zhong, U. von Sacken, J. Power Sources 54 (1995) 221.
[8] G.A. Nazri, A. Rougier, K.F. Kia, Mater. Res. Soc. Sym. Proc. 453 (1997) 635.
[9] M.K. Aydinol, A.F. Kohan, G. Ceder, K. Cho, J. Joannopoulos, Phys. Rev. B 56 (1997) 1354.
[10] G. Ceder, Y.-M. Chiang, D.R. Sadoway, M.K. Aydinol, Y.-I. Jang, B. Huang, Nature 392 (1998) 694.
[11] H.A. Lehmann, H. Hesselbarth, Z. Anorg. Allg. Chem. 313 (1961) 117.
[12] Y.-I. Jang, B. Huang, Y.-M. Chiang, D.R. Sadoway, Electrochem. Solid State Lett. 1 (1998) 13.
[13] Y.-M. Chiang, Y.-I. Jang, H. Wang, B. Huang, D.R. Sadoway, P. Ye, J. Electrochem. Soc. 145 (1998) 887.
[14] B. Huang, Y.-I. Jang, Y.-M. Chiang, D.R. Sadoway, J. Appl. Electrochem. 28 (1998) 1365.

[15] G. Ceder, unpublished work.
[16] H. Wang, Y.-I. Jang, B. Huang, D.R. Sadoway, Y.-M. Chiang, 81–82 (1999) 596–598.
[17] J. Morales, C. Pérez-Vicente, J.L. Tirado, Mater. Res. Bull. 25 (1990) 623.
[18] R.J. Gummow, M.M. Thackeray, Solid State Ionics 53–56 (1992) 681.
[19] E. Zhecheva, R. Stoyanova, Solid State Ionics 66 (1993) 143.
[20] T. Ohzuku, A. Ueda, M. Nagayama, J. Electrochem. Soc. 140 (1993) 1862.